FULL PAPER

Dalton
www.rsc.org/dalton

Coordinative flexibility of 1,2-bis[1,4,7-triazacyclonon-1-yl]propan-2-ol in mononuclear and binuclear Ni(II) complexes

Mark Warren,[a] Andrew R. Battle,[a] Boujemaa Moubaraki,[a] Keith S. Murray,[a] Leone Spiccia,*[a] Brian W. Skelton[b] and Allan H. White[b]

[a] *School of Chemistry, Monash University, Victoria, 3800, Australia. E-mail: leone.spiccia@sci.monash.edu.au; Fax: +61 3 99054597; Tel: +61 3 9905 4526*

[b] *School of Chemistry, University of Western Australia, Crawley, W.A., 6009, Australia*

Received 8th April 2004, Accepted 27th May 2004
First published as an Advance Article on the web 23rd June 2004

Reaction of 1,2-bis[1,4,7-triazacyclonon-1-yl]propan-2-ol hexabromide ($T_2PrOH.6HBr$) with $Ni(ClO_4)_2·6H_2O$ and adjustment of the pH to 7 resulted in the crystallization of pink and blue products from the one reaction mixture. The analytical data and X-ray structure determinations establish compositions corresponding to $[Ni(T_2PrOH)]Br(ClO_4)·H_2O$ (**1**, pink crystals) and $[Ni_2(T_2PrO)(OH_2)_3Br]Br(ClO_4)·2H_2O$ (**2**, blue crystals). A repeat synthesis of the latter yielded the diperchlorate monohydrate $[Ni_2(T_2PrO)(OH_2)_3Br](ClO_4)_2·H_2O$ (**3**). In the mononuclear complex (**1**), the 2-propanol group connecting the two 1,4,7-trizacyclononane (tacn) rings is protonated, the six nitrogen donors from the T_2PrOH ligand coordinating to a single Ni(II) centre in a distorted octahedral geometry. In the binuclear complexes (**2**) and (**3**), three coordination sites on each distorted octahedral Ni(II) centre are occupied *fac* by three nitrogen donors from the one tacn ring, the two metal centres being linked by an endogenous alkoxo bridge. A notable common feature of the two identical cations of (**2**) and (**3**) is that for one Ni(II) centre the remaining two sites are occupied by two water ligands, while in the other a bromo ligand replaces one ligated water. Similar binuclear systems have been recently defined $[Zn_2(T_2PrO)X(H_2O)_2](ClO_4)_2$ (X = Cl, Br), two complexes that exhibit coordination asymmetry with one pseudo-octahedral and one pseudo-square pyramidal Zn(II) centre. The weak antiferromagnetic coupling in **2** and **3** is discussed and compared to di-phenoxo-bridged Ni(II) examples.

Introduction

A recent publication has reported a pair of Cu(II) and Zn(II) complexes incorporating the deprotonated form of the binucleating ligand, 1,2-bis[1,4,7-triazacyclonon-1-yl]propan-2-ol (T_2PrOH).[1] Such examples of tacn derivatives which form polynuclear copper and zinc complexes with endogenous groups bridging the metal centers are comparatively rare.[2,3] For the Cu(II) complex, $[Cu_2(T_2PrO)Br_2]Br·2H_2O$, an X-ray structure determination and magnetic susceptibility measurements were undertaken to establish that the endogenous alkoxo bridge facilitates an antiferromagnetic exchange interaction between the two Cu(II) centres ($J = -86$ cm^{-1}). In the Zn(II) complex, $[Zn_2(T_2PrO)Br(H_2O)_2](ClO_4)_2$, an alkoxo bridge also connects the two Zn(II) centres but in this case coordination asymmetry was evident, 5- and 6-coordinate metal centres co-existing within each binuclear unit. A contemporaneous study by Morrow and co-workers[4] has reported the structure of the chloro analogue, $[Zn_2(T_2PrO)Cl(H_2O)_2](ClO_4)_2$, wherein the chloro ligand replaces the bromo ligand found in our complex. The observation of coordination asymmetry in both of these Zn(II) complexes formed by the T_2PrO^- ligand would suggest that this ligand has some influence as a determinant of the geometries of the Zn(II) centres. Despite the rarity of simple Zn(II) complexes exhibiting coordination asymmetry,[5–8] such a feature is quite common for Zn(II) centres found at the active sites of enzymes.[9] This somewhat unexpected structural feature of complexes formed by T_2PrO^- led us to explore the Ni(II) complexes formed by T_2PrO^- and the protonated form, T_2PrOH. We report here syntheses and X-ray structure determinations for three Ni(II) complexes, *viz*., a mononuclear bis(tacn) sandwich complex, $[Ni(T_2PrOH)]Br(ClO_4)·H_2O$ (**1**), and a pair of binuclear complexes, $[Ni_2(T_2PrO)(OH_2)_3Br]Br(ClO_4)·2H_2O$ (**2**) and $[Ni_2(T_2PrO)(OH_2)_3Br](ClO_4)_2·H_2O$ (**3**) in which the coordination spheres of the two Ni(II) centres are different.

Results and discussion

Synthesis

Two Ni(II) complexes, one incorporating T_2PrOH (LH) and the other the deprotonated T_2PrO^- (L) ligand were crystallised from an aqueous solution of $T_2PrOH·6HBr$ and $Ni(ClO_4)_2·6H_2O$ (1 : 4 ratio) whose pH had been adjusted to 7, slow evaporation yielding pink crystals of the sandwich complex, $[Ni(T_2PrOH)]Br(ClO_4)·H_2O$ (**1**), and blue crystals of the alkoxo bridged binuclear complex, $[Ni_2(T_2PrO)Br(H_2O)_3]Br(ClO_4)·2H_2O$ (**2**) that were suitable for X-structure determination. A deliberate synthesis of (**2**) in which a reaction mixture was allowed to evaporate at pH ~10 yielded the same binuclear cation but as its diperchlorate monohydrate $[Ni_2(T_2PrO)Br(H_2O)_3](ClO_4)_2·H_2O$ (**3**). This suggests that the mononuclear and binuclear complexes may be in equilibrium in solution as ionic aggregates which can be interconverted by pH adjustment. It is noteworthy that the conditions that initially yielded the mixture of **1** and **2** and subsequently **3** used an excess of nickel(II) perchlorate, excess nickel being precipitated as nickel hydroxide at pH 10. The observation that **3** is formed exclusively at pH 10 suggests the binuclear complex to be more stable at this pH in the presence of excess nickel, a reduction in pH to 7 inducing some rearrangement of the binuclear complex to the mononuclear sandwich complex, which crystallises from solution.

For the pink complex **1**, the IR spectrum shows a band at 3408 cm^{-1} attributed to the ν(OH) stretches of water in the crystal lattice and bands in the 3100–3350 cm^{-1} region which may be ascribed to ν(NH) stretches of the secondary amines in the ligand, together with the expected concomitant absorptions due to the ligand carbon framework and perchlorate counter-ions. Elemental analyses and the aqueous solution electrospray mass spectra showing peaks at *m*/*z* 186.1 ($[NiLH]^{2+}$), 372.2 ($[NiL]^+$), 453.1 ($[NiLHBr]^+$) 471.2 ($[NiLHClO_4]^+$) (L = T_2PrO^-) support the proposed constitution of the product. In the cases of **2** and **3**, strong OH (3422 cm^{-1}) and NH (3332 cm^{-1}) stretches are evident in the IR spectrum as well other ligand and counter-ion absorptions. The electrospray mass spectrum of **3** is consistent with a core structure of $[Ni_2L]$, the complex losing water ligands, and exhibiting peaks at *m*/*z* of 241.1, 264.9 and 525 corresponding to $[Ni_2LBr]^{2+}$, $[Ni_2L(ClO_4)]^{2+}$ and $[Ni_2L(Br)(OH)]^+$, respectively. Microanalysis of **3** supports the formulation $[Ni_2(T_2PrO)Br(H_2O)_3](ClO_4)_2·H_2O$, the structure being confirmed by a single crystal X-ray crystallographic study.

Crystal structures

The results of the single crystal X-ray structure determinations are consistent with the formulations of the compounds as

DOI: 10.1039/b405320f

Table 1 Selected geometries, $[NiLH]^{+a}$

Atom	*r*	N(14)	N(17)	N(21)	N(24)	N(27)
N(11)	2.150(5)	84.4(2)	81.2(2)	92.7(2)	173.8(2)	104.4(2)
N(14)	2.100(6)		81.5(2)	172.6(2)	99.2(2)	91.7(2)
N(17)	2.152(6)			104.8(2)	94.3(2)	170.8(2)
N(21)	2.123(5)				84.3(2)	82.4(2)
N(24)	2.100(6)					80.6(2)
N(27)	2.155(6)					

[a] The metal environment: *r* (Å) is the Ni–N distance, the other entries being the angles subtended by the relevant atoms at the head of the row and column. Torsion angles in the tacn rings, given around each ring, beginning with the N(n1)–C(n2) bond: −65.5(3), −47.5(7), 133.9(6), −71.7(7), −42.0(8), 132.3(6), −75.4(7), −45.2(7), 131.4(6) (ring 1); −67.7(7), −48.7(8), 139.2(6), −69.0(7), −41.3(8), 131.8(6), −81.7(7), −36.4(8), 125.1(6)° (ring 2). In the six-membered bridging ring, torsions in the bonds outward to either side of C(0) are: 45.8(9), 21.5(2); −64.0(7), −56.6(7); 24.8(5), 30.6(5)° (*i.e.*, a 'boat').

$[NiLH]Br(ClO_4)\cdot H_2O$ (**1**), $[Ni_2LBr(OH_2)_3]Br(ClO_4)\cdot 2H_2O$ (**2**), and $[Ni_2LBr(OH_2)_3](ClO_4)_2\cdot H_2O$ (**3**), respectively. Projections of the mononuclear cation (**1**) and the dinuclear cation (**2**) are shown in Figs. 1 and 2. Bond distances and angles for **1** are reported in Table 1, while those for **2** and **3** are shown in Table 2.

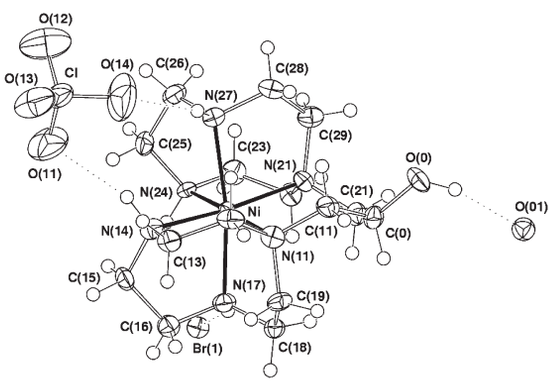

Fig. 1 Projection of the mononuclear $[NiLH]^{2+}$ cation of **1** with associated hydrogen bonded moieties.

The geometries of the $[Ni_2LBr(OH_2)_3]^{2+}$ complex cations of **2** and **3** generally do not differ, the most significant exception being that the Ni(1)–O(1)–Ni(2) angle in **3** (137.8(1)°) is less acute than that in **2** (136.6(1)°). In **2** and **3**, a binuclear cation together with companion counterions, devoid of crystallographic symmetry, comprise the asymmetric unit in each case. In each $[Ni_2LBr(OH_2)_3]^{2+}$ cation, the oligodentate ligand, comprised of two similar halves about the central C–O bond, embraces one metal atom within each half, the (anionic) oxygen atom bridging them. Each half of the ligand occupies four coordination sites about the metal, the three nitrogen atoms of the tacn ring *fac* in the coordination sphere. The coordination spheres are six-coordinate with the anionic bridging-*O* and the tertiary nitrogen of the ligand (associated with the longest M–N distance in each case) quasi-*trans*/'axial', although the associated angles are considerably reduced from 180°. Both metal atoms are six-coordinate, one with a (Br + H_2O) unidentate complement, the other 2 × H_2O. While this may be considered an extension of the recently reported zinc cation situation,[1,4] in the sense that the Ni(II) complex differs from the Zn(II) complex through an augmentation of the coordination number of one metal centre (M(2) by one (further water molecule), a further difference is that the coordination sphere of M(1) is rearranged so that the bromide ligand, *trans* to N(11) in the zinc complex, is interchanged with the aqua ligand, the changes impacting on the metal atom environment geometries in the expected manner.

In the mononuclear species, the ligand, now protonated, embraces the six-coordinate metal through its pair of N_3-triamine rings, the protonated oxygen uncoordinated: $[NiLH]^{2+}$. The two triaza rings have the same chirality and conformation, the latter being similar to those in **2** and **3**; except for the disparity in substituents at C(0), the cation is a good approximation to 2-symmetry. The ligand disorder

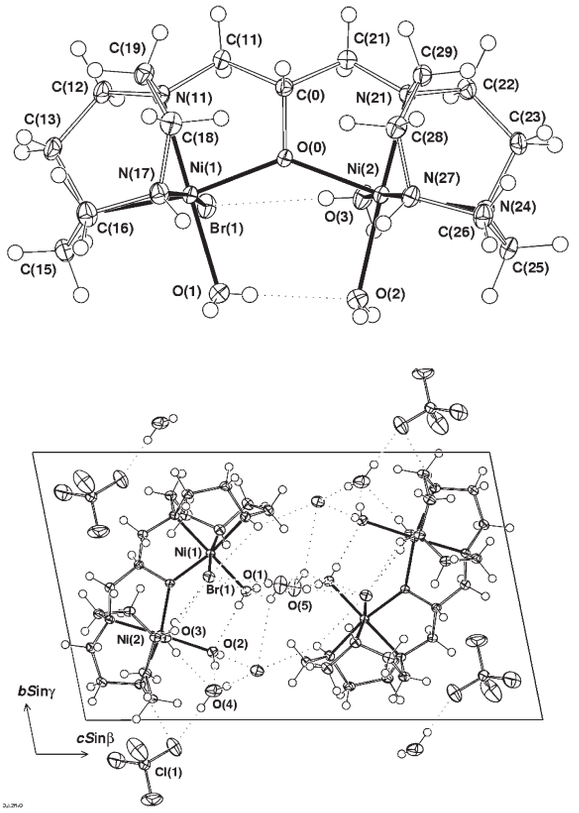

Fig. 2 Projection of the binuclear cation of **2** (that of **3** is similar) showing intracation hydrogen bonding (top). Unit cell of **2** projected down the *a* axis showing hydrogen bonded columns (bottom).

noted previously in the copper complex, $[Cu_2LBr_2]Br\cdot 2H_2O$,[1] is absent in the present binuclear nickel counterparts. Here, however, the ligand symmetry is quite different, being a good approximation to 2 overall, compatible with an achievable non-disordered ligand conformation, but broken in the cation more widely by the impact of the differences (again) in the metal atom coordination environments, as found in the zinc complex.[1,4] Thus while the individual cation of the copper complex is inherently chiral, because of the ligand disposition, that of the nickel complex is only so by virtue of the different metal atom coordination environments. As well as the torsion angles of the two tacn rings being of opposite sign, the divergences between the various 'equivalent' parameters of the ligand in the zinc complex are rather greater than in the nickel complex reported here. The tacn rings throughout all compounds, taken by themselves, have their usual quasi-3-symmetry.

In **2** interesting interactions between coordinated species are observed: Br(1)···H(3a) is 2.47(6), and H(1a)···O(2) 2.13(6) Å; there is another close contact to the bromide from a lattice water molecule: Br(1)···H(5a)(O(5)) 2.3_6 (est.) (3.198(2) Å), while Br(2)···H(4b) (1 − *x*, 1 − *y*, 1 − *z*) is 2.31(5) Å. Other short contacts are found from the coordinated to the lattice water molecules: H(1b)···O(5) (1 − *x*, 1 − *y*, 1 − *z*) 1.81(5); H(2a)···O(4) 1.92(4), H(3b)···O(4) 2.08(5), with H(4a)···O(11)(perchlorate) 1.93(5) Å. In the mononuclear complex, **1**, the disordered components of the lattice water are equidistant from the alcohol: O,H(0)···O(01,02) (*x* − 1/2, 1/2 − *y*, *z* − 1/2) 2.81(1), 2.88(1); 1.8_6, 1.9_9 Å (est.), while H(n4,7) of the ligand exhibit stronger, more well-defined interactions with the major component of the perchlorate and bromide: H(14)···O(11), H(24)···O(14) 2.2 Å (X2), H(17)···Br 2.5 Å (all est.), cation/anion aggregates lying in columns up the *a* axis (Fig. 2(b)).

In **3**, the cation is the same as that of **2**, albeit less well defined, intracation hydrogen bonding, as a consequence of disorder within the structure, affecting one of the perchlorate anions: further afield, hydrogen-bonding between cations and anions results in a layered structure within the lattice (Fig. 3).

The single oxygen Ni–O–Ni bridge of **3** gives rise to a M···M distance of 3.813(2) Å, which is slightly longer than that of **2**

Table 2 Nickel(II) atom environments in **2** and **3**

	Ni/1 (**2**)	Ni/2[a] (**2**)	Ni/1 (**3**)	Ni/2 (**3**)[a]
Distance/Å				
M(n)–O(0)	2.039(3)	2.050(2)	2.031(2)	2.055(3)
M(n)–N(n1)	2.060(2)	2.065(2)	2.063(3)	2.060(3)
M(n)–N(n4)	2.082(2)	2.103(2)	2.080(3)	2.107(3)
M(n)–N(n7)	2.097(2)	2.077(2)	2.077(3)	2.081(3)
M(n)–Br(n)	2.8038(5)	2.100(2)	2.8412(9)	2.124(3)
M(n)–O(n)	2.019(2)	2.131(2)	2.077(3)	2.146(3)
Angle/degree				
M(n)–O(0)–M(n′)	136.6(1)	—	137.8(1)	—
M(n)–O(0)–C(0(,0′))	110.7(1)	111.1(1)	110.0 (2)	111.2(2)
M(n)–N(n1)–C(n1)	103.4(2)	103.6(2)	103.9(2)	104.5(2)
M(n)–N(n1)–C(n2)	104.9(2)	104.6(2)	105.2(2)	105.5(2)
M(n)–N(n1)–C(n9)	109.6(2)	108.3(2)	109.2(2)	108.5(2)
C(n1)–N(n1)–C(n2)	113.6(2)	113.1(2)	113.4(2)	113.2(3)
C(n1)–N(n1)–C(n9)	112.5(2)	112.9(2)	112.1(3)	112.1(3)
C(n2)–N(n1)–C(n9)	112.2(2)	113.4(2)	112.4(3)	112.5(3)
M(n)–N(n4)–C(n3)	108.8(2)	108.7(2)	109.6(2)	109.6(2)
M(n)–N(n4)–C(n5)	105.3(2)	105.0(1)	104.6(2)	104.4(2)
C(n3)–N(n4)–C(n5)	114.1(2)	113.6(2)	113.9(3)	114.1(3)
M(n)–N(n7)–C(n6)	110.4(2)	110.6(1)	109.8(2)	111.2(3)
M(n)–N(n7)–C(n8)	104.6(2)	104.0(2)	105.6(2)	103.5(2)
C(n6)–N(n7)–C(n8)	113.1(2)	113.7(2)	113.5(3)	113.4(3)
O(0)–M(n)–Br(n)	91.34(5)	86.87(8)	90.28(7)	87.9(1)
O(0)–M(n)–O(n)	94.75(8)	98.25(8)	96.2(1)	96.4(1)
O(0)–M(n)–N(n1)	84.90(8)	83.63(8)	84.8(1)	83.4(1)
O(0)–M(n)–N(n4)	168.95(9)	167.22(9)	167.3(1)	166.7(1)
O(0)–M(n)–N(n7)	99.85(8)	100.09(8)	101.8(1)	99.4(1)
Br(n)–M(n)–N(n1)	96.23(6)	95.20(9)	96.86(8)	95.2(1)
Br(n)–M(n)–N(n4)	86.11(6)	90.05(8)	84.72(9)	90.1(1)
Br(n)–M(n)–N(n7)	168.80(6)	173.03(9)	168.01(9)	172.8(1)
Br(n)–M(n)–O(n)	84.07(7)	84.67(9)	85.37(9)	87.0(1)
O(n)–M(n)–N(n1)	179.5(1)	178.10(9)	177.5(1)	177.7(1)
O(n)–M(n)–N(n4)	95.7(1)	93.81(9)	95.0(1)	96.6(1)
O(n)–M(n)–N(n7)	95.3(1)	94.4(1)	93.1(1)	92.4(1)
N(n1)–M(n)–N(n4)	84.69(9)	84.30(9)	84.2(1)	83.7(1)
N(n1)–M(n)–N(n7)	84.47(9)	85.50(9)	84.5(1)	85.4(1)
N(n4)–M(n)–N(n7)	82.83(9)	83.11(8)	83.1(1)	82.8(1)

[a] For Br(n) read O(3).

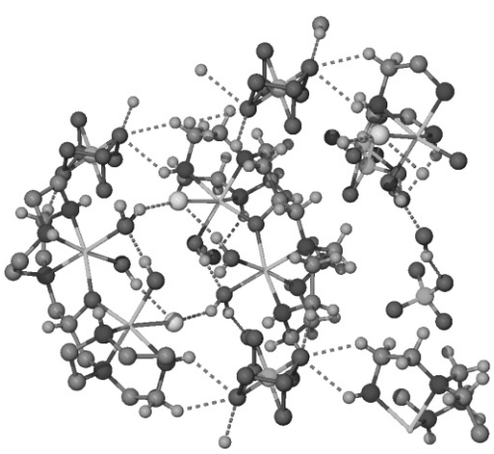

Fig. 3 Povray representation of the hydrogen bonding network in **3**.

(3.782(5) Å), as a result of the less acute Ni–O–Ni angle. Both these distances are longer than those observed in the Cu(II) and Zn(II) analogues (3.582(1) and 3.684(1) Å, respectively)[1,4] and in an oxo- and hydroxo-bridged tetranuclear iron cluster incorporating the same ligand (Fe···Fe separations 3.510(2) and 3.513(2) Å).[10]

Magnetic properties

The dinuclear complex **3** displays characteristic antiferromagnetic coupling with a maximum susceptibility at 47 K, the rapid increase at very low temperatures being due to the ubiquitous monomer impurity (Fig. 4). The corresponding $\chi_M T$ values decrease accordingly from 1.03 cm^3 mol^{-1} K (2.87 μ_B) per Ni at 300 K to 0.17 cm^3 mol^{-1} (1.17 μ_B) at 12 K. Fitting to a $-2J\boldsymbol{S}_1\boldsymbol{S}_2$ Heisenberg model for $S_1 = S_2 = 1$ gave an excellent fit when the following parameters were employed; $g = 2.10$, $J = -17.7$ cm^{-1}, % monomer = 3.8, temperature independent paramagnetism ($N\alpha$) = 120×10^{-6} cm^3 mol^{-1}. Complex **2** behaves similarly to **3** but with the maximum in χ_M at 32 K indicating weaker antiferromagnetic coupling. The best-fit parameters were $g = 1.94$, $J = -12.6$ cm^{-1}, % monomer = 6.7 and $N\alpha = 120 \times 10^{-6}$ cm^3 mol^{-1}. The small difference in the J values for **2** and **3** presumably reflect the small difference in Ni···Ni separation and Ni–O–Ni bridge angle (*vide infra*), but might also be influenced indirectly by inter-dimer H-bonding effects. There are few alkoxo bridged nickel(II) systems to permit a comparison of J values, most such examples possessing square planar Ni(II) centres, and so being diamagnetic.[11] Some discrete phenoxo-bridged dinuclear[11–13] and tetranuclear[14] complexes have J values in the range −23 cm^{-1} to −20 cm^{-1}, somewhat higher than in **3**. These systems have Ni···Ni separations of approximately 3.1 Å, Ni–O–Ni angles of 96–100°, and trigonal planar oxygen bridges. In comparison, **3** has a longer Ni···Ni separation of 3.813(2) Å, a corresponding larger bridge angle of 137.8(2)° and a trigonal planar O(0) bridging corners of two octahedra. Thus it appears that this simple bridge is as effective at transmitting exchange coupling as are a pair of phenoxo-oxygens bridging the edges of two octahedra. Another alkoxo-bridged (tetranuclear) complex displayed ferromagnetic coupling ($J = +10.6$ cm^{-1}) but this involves a second μ-1,1-azide bridging group,[15] notable for resulting in net ferromagnetic coupling.

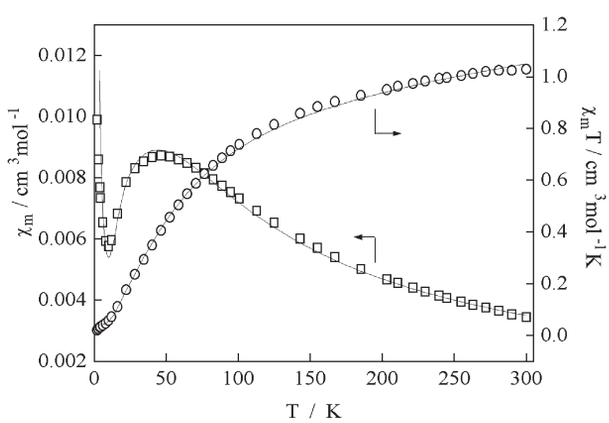

Fig. 4 Plot of χ_m (per Ni) and $\chi_m T$ (per Ni) *versus* temperature for **3**.

Experimental

Materials

Commercial chemicals and solvents were of reagent grade quality or better and were used as received. T_2PrOH·6HBr was prepared by the method of Wieghardt and co-workers.[16]

Physical measurements

Electrospray ionization (ESI) mass spectra were recorded on a Micromass Platform quadrupole mass spectrometer or a Bruker BioApex 47e Fourier Transform mass spectrometer. Quoted *m*/*z* values refer to the most intense peak present in each signal envelope. IR spectra were recorded using KBr disks on a Perkin-Elmer 1600 series FTIR spectrophotometer. Solid state diffuse reflectance UV-Visible-NIR were measured on a Cary 5G instrument.

Magnetic measurements

Magnetic measurements were carried out on a Quantum Design MPMS 5 SQUID magnetometer calibrated using a standard palladium sample (Quantum Design) of accurately known magnetisation or magnetochemical calibrants such as $CuSO_4 \cdot 5H_2O$. Susceptibility *vs.* temperature studies in the linear portion of the magnetisation *vs.* field curve were made using a field of 1 T. A powdered sample

(2.4 mg for **2** and 20 mg for **3**) was contained in a calibrated gelatine capsule held at the centre of a drinking straw fixed to the end of the sample rod.

Syntheses

[NiLH]Br(ClO_4)·H_2O (1, pink), [$Ni_2LBr(OH_2)_3$]Br(ClO_4)·$2H_2O$ (2, blue) and [$Ni_2LBr(OH_2)_3$](ClO_4)$_2$·H_2O (3, blue)

$Ni(ClO_4)_2·6H_2O$ (0.186 g, 0.5 mmol) was dissolved in 10 ml of distilled water with the pH adjusted to 6 with 1 M NaOH. The ligand, T_2PrOH.6HBr (0.100 g, 0.127 mmol) was dissolved in 5 ml of water and added to the nickel(II) perchlorate solution with the pH adjusted to 10 with 1 M NaOH. The resulting solution was filtered to remove the precipitated nickel(II) hydroxide and the pH of the filtrate adjusted to 7 with 1 M HBr. The filtrate was then allowed to slowly evaporate at room temperature yielding a mixture of blue and pink crystals, which were then separated. Yield (pink crystals, **1**, 0.010 g; 14%; blue crystals, **2**, 0.011 g, 11%. The blue compound **3** was formed by reacting $Ni(ClO_4)_2·6H_2O$ (0.188 g, 0.5 mmol), dissolved in 10 ml of water, with T_2PrOH.6HBr (0.050 g, 0.064 mmol), dissolved in 5 ml of water, and adjustment of the pH to 10 with 1 M NaOH. The solution was filtered to remove the nickel(II) hydroxide precipitate and allowed to slowly evaporate at room temperature. Yield of **3**, 0.030 g, 60%.

Analyses. *1*. Found: C 29.9, H 5.6, N 14.1%. Calc. for [NiLH]$BrClO_4·H_2O$ ($C_{15}H_{36}BrClN_6NiO_6$): C 31.6, H 6.4, N 14.7%. Calc. for [NiLH]$BrClO_4·2H_2O$ ($C_{15}H_{38}BrClN_6NiO_7$): C 30.6, H 6.5, N 14.3%. Electrospray mass spectrum (aqueous) +ve ion: *m*/*z* 186.1 (100%, $[NiLH]^{2+}$), 372.2 (5%, $[NiL]^+$), 453.1 (5%, $[NiLHBr]^+$) 471.2 (5%, $[NiLHClO_4]^+$); −ve ion 612.9 (50%, $[NiLHBr_3]^-$). IR spectrum (KBr; *ν*, cm^{-1}): 3407s, 3335m, 3265s, 3110m, 2905m, 2875m, 1624w, 1489m, 1364w, 1305w, 1283w, 1102vs, 1024s, 996m, 952m, 888w, 822w, 625m.

2. Full analysis of **2** could not be carried out because of the small sample size and co-crystallization of inorganic salts with the binuclear complex. Found: C 20.1, H 3.1, N 9.6% Calc. For [$Ni_2LBr(OH_2)_3$]Br(ClO_4)·$2H_2O$ ($C_{15}H_{43}Br_2ClN_6Ni_2O_{10}$): C 23.0, H 5.5, N 10.8% Calc. for [$Ni_2LBr(OH_2)_3$]Br(ClO_4)·$NaClO_4$ ($C_{15}H_{39}Br_2Cl_2N_6Ni_2NaO_{12}$): C 20.8, H 4.5, N 9.7%

3. Found C 22.6, H 5.1, N 10.3% Calc. for [$Ni_2LBr(OH_2)_3$](ClO_4)$_2$·H_2O, ($C_{15}H_{41}BrCl_2N_6Ni_2O_{13}$) C 23.1, H 5.3. N 10.8%. Electrospray mass spectrum (aqueous) +ve ion: *m*/*z* 241.09 (70% $[NiLBr]^{2+}$), 264.9 (20% $[NiL(ClO_4)]^{2+}$), 525.1 (5% $[NiL(Br)(OH)]^+$). Diffuse reflectance UV-Vis-NIR spectrum: (λ_{max}, nm) 589, 378. IR spectrum (KBr; *ν*, cm^{-1}): 3422s, 3332m, 2932m, 2893s, 1655w, 1626w, 1494w, 1461m, 1360w, 1108s, 1006m, 945m, 892w, 869w, 827w, 657w, 626m.

Structure determinations

For **1** and **2**, full spheres of CCD area-detector diffractometer data were measured (Bruker AXS instrument, *ω*-scans; monochromatic Mo Kα radiation ($\lambda = 0.7107_3$ Å); *T ca.* 153 K). $N_{t(total)}$ reflections were obtained, merging to *N* unique (R_{int} cited) after 'empirical'/multiscan absorption correction (proprietary software), N_o with $F > 4\sigma(F)$ being used in the full matrix least squares refinements. Anisotropic thermal parameter forms were refined for the non-hydrogen atoms, $(x, y, z, U_{iso})_H$ being treated as described below. Conventional residuals *R*, R_w on |*F*| are quoted at convergence (weights: $(\sigma^2(F) + 0.0004F^2)^{-1}$). Neutral atom complex scattering factors were employed within the Xtal 3.7 program system.[17] Data for **3** were measured on an Enraf-Nonius Kappa instrument at 123(2) K using phi and/or omega scans. The structure was solved by direct methods and refined using the full matrix least-squares method of the programs SHELXS-97 and SHELXL-97,[18] respectively, the program X-Seed[19] being used as an interface to the SHELX programs. Pertinent results are given below and in the tables and figures, the latter showing 50% probability displacement ellipsoids for the non-hydrogen atoms, hydrogen atoms having arbitrary radii of 0.1 Å.

CCDC reference numbers 235854–235856.

See http://www.rsc.org/suppdata/dt/b4/b405320f/ for crystallographic data in CIF or other electronic format.

Crystal/refinement data. *1*. [NiLH]Br(ClO_4)·H_2O (pink) ≡ $C_{15}H_{36}BrClN_6NiO_6$, *M* = 570.5. Monoclinic, space group $P2_1/n$, $a = 11.351(1)$, $b = 16.545(2)$, $c = 11.618(1)$ Å, $\beta = 90.604(2)°$, $V = 2182$ Å^3. D_c ($Z = 4$) = 1.73_7 g cm^{-3}. $\mu_{Mo} = 29$ cm^{-1}; specimen: 0.13 × 0.10 × 0.05 mm; 'T'$_{min/max} = 0.84$. $2\theta_{max} = 50°$; $N_t = 35308$, $N = 3825$ ($R_{int} = 0.085$), $N_o = 3141$; $R = 0.068$, $R_w = 0.11$.

Variata. $(x, y, z, U_{iso})_H$ were constrained throughout at (difference map) estimates, except those for the lattice water molecule oxygen (which was modelled as disordered over a pair of sites set at equal occupancy) which were not located. The uncoordinated anions were modelled as disordered in concert over two sets of sites, occupancies refining to 0.929(6) and complement, the perchlorate rotationally disordered about a Cl–O bond. The bulk material was badly twinned, the data being measured on a small chip.

2. [$Ni_2LBr(OH_2)_3$]Br(ClO_4)·$2H_2O$ (blue) ≡ $C_{15}H_{43}Br_2ClN_6Ni_2O_{10}$, *M* = 780.2. Triclinic, space group $P\bar{1}$, $a = 7.4997(7)$, $b = 10.926(1)$, $c = 17.743(2)$ Å, $\alpha = 100.661(2)$, $\beta = 91.129(2)$, $\gamma = 102.496(2)°$, $V = 1392$ Å^3. D_c ($Z = 2$ fu) = 1.86_1 g cm^{-3}. $\mu_{Mo} = 44$ cm^{-1}; specimen: 0.35 × 0.22 × 0.11 mm; 'T'$_{min/max} = 0.57$. $2\theta_{max} = 70°$; $N_t = 25646$, $N = 12204$ ($R_{int} = 0.049$), $N_o = 8941$; $R = 0.044$, $R_w = 0.055$.

Variata. $(x, y, z, U_{iso})_H$ were refined throughout except for those associated with lattice water 5 which were constrained at sites estimated from difference maps.

3. [$Ni_2LBr(OH_2)_3$](ClO_4)$_2$·H_2O (blue) ≡ $C_{15}H_{41}BrCl_2Ni_2O_{13}$, *M* = 781.77, Triclinic, space group $P\bar{1}$, $a = 9.3686(19)$, $b = 11.204(2)$, $c = 14.198(3)$ Å, $\alpha = 79.66(3)$, $\beta = 86.68(3)$, $\gamma = 78.68(3)°$, $V = 1437$ Å^3. D_c ($Z = 2$ fu) = 1.80_6 g cm^{-3}. $\mu_{Mo} = 30$ cm^{-1}; specimen: 0.25 × 0.4 × 0.2 mm; 'T'$_{min} = 0.3844$. 'T'$_{max} = 0.5895$. $2\theta_{max} = 55°$; $N_t = 20593$, $N = 6776$ ($R_{int} = 0.065$); $R = 0.041$, $R_w = 0.1130$.

Variata. $(x, y, z, U_{iso})_H$ were refined for the coordinated water molecules, water of solvation and the secondary nitrogens, but were constrained at estimates at all other sites. One perchlorate anion was refined at full occupancy, the other anion being disordered and modelled over two sites, each at half occupancy.

Acknowledgements

This work was supported by the Australian Research Council.

References

1 F. H. Fry, B. Moubaraki, K. S. Murray, L. Spiccia, M. Warren, B. W. Skelton and A. H. White, *Dalton Trans.*, 2003, 866.
2 H. Weller, L. Siegfried, M. Neuburger, M. Zehnder and T. A. Kaden, *Helv. Chim. Acta*, 1997, **80**, 2315.
3 S. J. Brudenell, L. Spiccia, D. C. R. Hockless and E. R. T. Tiekink, *J. Chem. Soc., Dalton Trans.*, 1999, 1475.
4 O. Iranzo, A. Y. Kovalesky, J. R. Morrow and J. P. Richard, *J. Am. Chem. Soc.*, 2003, **125**, 1988.
5 T. Tanase, J. W. Yun and S. J. Lippard, *Inorg. Chem.*, 1995, **34**, 4220.
6 H. Adams, D. Bradshaw and D. E. Fenton, *Polyhedron*, 2002, **21**, 1957.
7 S. R. Korupoju, N. Mangayarkarasi, P. S. Zacharias, J. Mizuthani and H. Nishihara, *Inorg. Chem.*, 2002, **41**, 4099.
8 H. Adams, D. Bradshaw and D. E. Fenton, *J. Chem. Soc., Dalton Trans.*, 2001, 3407.
9 W. N. Lipscomb and N. Sträter, *Chem. Rev.*, 1996, **96**, 2375; N. Sträter, W. N. Lipscomb, T. Klabunde and B. Krebs, *Angew. Chem., Int. Ed. Engl.*, 1996, **35**, 2025; D. E. Wilcox, *Chem. Rev.*, 1996, **96**, 2435.
10 J. L. Sessler, J. W. Sibert, A. K. Burrell, V. Lynch, J. T. Markert and C. L. Wooten, *Inorg. Chem.*, 1993, **32**, 4277.
11 M. Kwiatkowski, E. Kwiatkowski, O. Olechnowicz, D. M. Ho and E. Deutsch, *J. Chem. Soc., Dalton Trans.*, 1990, 3063.

12 S. L. Lambert and D. N. Hendrickson, *Inorg. Chem*, 1979, **18**, 2683.
13 C. L. Spiro, S. L. Lambert, T. J. Smith, E. N. Duesler, R. R. Gagne and D. N. Henrickson, *Inorg. Chem.*, 1981, **20**, 1229.
14 A. J. Edwards, B. F. Hoskins, E. H. Kachab, A. Markiewicz, K. S. Murray and R. Robson, *Inorg. Chem.*, 1992, **31**, 3585.
15 J. Ribas, M. Monfort, R. Costa and X. Solans, *Inorg. Chem.*, 1993, **32**, 695.
16 K. Wieghardt, I. Tolksdorf and W. Herrmann, *Inorg. Chem.*, 1985, **24**, 1230.
17 *The Xtal 3.7 System*, ed. S. R. Hall, D. J. du Boulay and R. Olthof-Hazekamp, University of Western Australia, Perth, 2001.
18 G. M. Sheldrick, *SHELXL-97*, University of Göttingen, Germany, 1997.
19 L. J. Barbour, X-Seed—A software tool for supramolecular crystallography, *J. Supramol. Chem.*, 2001, **1**, 189.